EPJ manuscript No.
(will be inserted by the editor)

Spin Interactions and Cross-checks of Polarization in NH_3 Target

Yu. Kiselev[1,a], G. Baum[2], N. Doshita[3], F. Gautheron[1,2], Ch. Hess[1], T. Iwata[3], J. Koivuniemi[1], K. Kondo[3], A. Magnon[4], G. Mallot[5], T. Michigami[3], W. Meyer[1], and G. Reicherz[1]

[1] Physics Department, University of Bochum, 44780 Bochum, Germany
[2] Physics Department, University of Bielefeld, 33501 Bielefeld, Cermany
[3] Department of Physics, Faculty of Science, Yamagata University, 990-8560, Yamagata, Japan
[4] CEA Saclay, DAPNIA, 91191 Gif-sur-Yvette, France
[5] CERN, 1211 Geneva, Switzerland

Abstract. We study the magnetic structure of irradiated ammonia (NH_3) polarized by Dynamic Nuclear Polarization method at 0.2 K and at 2.5 T field. In this material, the electron spins, induced by ionizing radiation, couple ^{14}N and ^1H spins by the indirect spin-spin interaction. As a result, the local frequencies of ^1H-spins are varied depending on ^{14}N spin polarizations and lead to an asymmetry in the proton signal. This asymmetry allowes a good detection of ^{14}N spins directly on the proton Larmor frequency. In the long COMPASS target at CERN, we use the cross-checks between spectral asymmetries and integral polarizations to decrease the relative error for longitudinal target polarizations up to $\pm 2.0\%$.

1 Introduction

The history of irradiated target materials is well presented in reports [1,2]. It was shown, that the highest polarizations are reached by Dynamic Nuclear Polarization (DNP) method which requires the presence of paramagnetic dopant. The optimal irradiation dose should induce $(2 \div 5) \cdot 10^{19}$ spin/cm^3 concentration of electron spins to reach the highest polarizations. The intense studies and new developments demonstrated the availability of high nuclear polarizations in irradiated $^{14}NH_3$, $^{15}NH_3$, $^{14}ND_3$ and $^{15}NH_3$ [3].

There are less studied aspects of the ionizing technique deserving of more systematic consideration. Irradiation can produce the free electron spins in any dielectric material that is important for its wide practical applications. Unlike chemically stable radicals also used in DNP, beam induced spins are not screened by surround molecules; their quasi-stable state is supported only due to cooling down lower than 90 K [2]. Such spins tend to have nonzero electron densities at the sites of surrounding nuclei, therefore they induce a specific coupling between nuclear spin species, so-called indirect spin-spin interactions [4].

We propose to use indirect interactions, induced by beam, for the study of dielectrics and perhaps biological media at super-low temperatures. Following our logic, the asymmetry of proton spectra, for instance in $^{14}NH_3$, caused by indirect coupling with ^{14}N spins, can be itself used as a detector of ^{14}N spins. Irradiated ammonia [5], investigated in this paper, is a good example for future analysis of small gyromagnetic ratios and rare nuclei by this method.

Herein, the influence of beam induced indirect coupling on the magnetic structure of ammonia, on the local field and on the signal asymmetry is shown. We compare NMR nitrogen spectra with their "impressions" in the proton spectra owing to indirect coupling. As for applications,

[a] e-mail: Yury.kiselev@cern.ch

we tested the correlation between proton line asymmetries and their integral polarizations in different Q-meter probes along the COMPASS target at CERN. This cross-check allows better accuracy for the polarization measurement.

2 Material for DNP and Setup equipment

2.1 Three cell COMPASS target

Our data were obtained from the COMPASS target at CERN made of irradiated NH_3-ammonia. The target consists of the three cells (30+60+30) cm long and 4 cm in diameter, filled with granulated material. It operates at 2.5 T field, with microwaves (MW) of $\lambda \cong 4$ mm wavelength in the temperature range from 0.06 to 0.25 K. The nuclear polarization is measured by ten commercial "Liverpool" Q-meters [6] connected to probing coils equally distributed along the target. The receiver circuits were permanently tuned to ν_0=106.42 MHz and fed by a RF synthesizer, the frequency was scanned 1000 frequency steps across the frequency center with 600 kHz bandwidth.

2.2 Features of irradiated ammonia

Target material was prepared almost 15 years ago by irradiation at the Bonn University using the 20 MeV electron linac [7]. During the irradiation the sample was kept in liquid argon at 87 K (high temperature irradiation). The electron beam current was typically 2×10^{14} e^-/s, an accumulated flux of 10^{17} e^-/cm^2 obtained in 2.5 hour [3]. The first visible result for an irradiated ammonia is the violet color of the material. The intensity of this color depends on the irradiation dose and is a scale for the radical density. Proton polarization were reached routinely by DNP method; the highest polarization of $\pm(98 \pm 2.0)\%$ for the freshly produced ammonia (see [3]) and of $\pm(94 \pm 2.5)\%$ after its long storage, see Fig. 5(b)).

At room temperature, radicals have only a volatile existence because they react very rapidly either with themselves or with other molecules. However, at liquid N_2 temperatures they are more or less stable. After some years the $^{14}NH_3$ material, kept under liquid N_2, became paler, thus indicated a loss of radicals, and its efficiency for target applications is lowered. One of possible amine radical $^{14}\dot{N}H_2$ completely disappears at temperatures higher than 117 K.

The first measurements of nuclear polarizations were done by Adeva and al. [7]; a simple model for proton line-shape was developed in order to study the nonlinear corrections of Q-meter. After almost ten years, we again recommenced the study of the same material because, during its long storage at liquid nitrogen, the electron concentration had strongly decayed. The comparison between the perfomances freshly produced and of old material motivated us to make its magnetic structure more exact and to propose new practical applications of beam irradiation for the study of rare and quadrupole nuclei.

3 Spin structure of irradiated $^{14}NH_3$-ammonia

3.1 Beam induced J-interaction

Typical proton NMR signals in an amorphous solid NH_3 are shown in 1(a) for low and high, positive and negative polarizations [7]. We neglect small line shape broaden due to the inhomogeneous external field, which is on the order of 5×10^{-5}.

At low polarizations, the spectra have a symmetrical line shape about the Larmor frequency ν_0, broadened by dipolar interactions. The symmetry comes from the fact that dipolar interaction do not depend on the spin permutations and that the NH_3-group is relatively isolated [8].

At higher polarizations, the line shape become strongly asymmetric and it is shifted by the local field in different directions depending on the sign of proton polarization $P_\pm$. The local

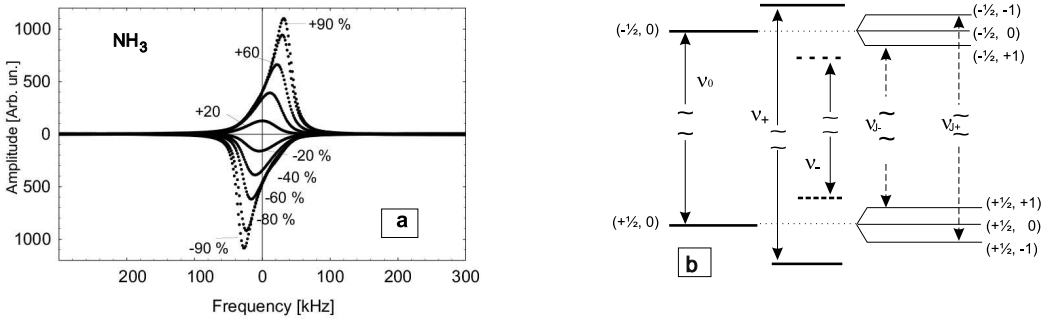

Fig. 1. a) Proton NMR-spectra for approximately ±20%, ±40%, ±60%, ±80% and ±90%; the fresh sample [7]. b). (m_p,m_n)-transitions in NH_3: ν_0-Larmor frequency, ν_+, ν_- are the frequencies shifted by H_{loc} at opposite signs of polarizations; ν_{J+} and ν_{J-}-are J-coupling transitions.

field H_{loc} equals to the first moment of the proton line shape, which is the linear combination of spin system parameters [9,10]

$$H_{loc}[Gauss] = \frac{2\pi}{3}h(3\gamma_p N_p I_p P_p + 2\gamma_n N_n I_n P_n) \approx 2\pi h \gamma_p N_p I_p P_p, \quad (1)$$

where h is the Plank's constant; indexes p and n stand for ^{1}H and for ^{14}N spins, $\gamma_{p,n}$, $I_{p,n}$, $N_{p,n}$, $P_{p,n}$ are the gyromagnetic ratios, spins, densities and nuclear polarizations, respectively. Since $\gamma_p \setminus \gamma_n \approx 14$, $P_p \gg P_n$ and $N_p = 3 \cdot N_n$ we neglect the second term in Eq. 1, therefore the energy of polarized protons ($I_p = 1/2; m_p = \pm 1/2$) in a external magnetic field H_0 is

$$E_p = -h\gamma_p(H_0 + H_{loc})m_p \ , \quad (2)$$

Fig. 1(b) shows ν_+ and ν_- transitions for opposite polarizations shifted by H_{loc} with respect to ν_0=$\gamma_p H_0$. Previous analysis [7] supposed an equal influence of local field onto all proton spins in ammonia. Let's analyse this assumption in detail. The line shapes of oppositely polarized protons are shown in Fig. 2(a). Data in Fig. 2(a,b) show $\delta 1$ center and $\delta 2$ maximum signal displacements over proton polarization, where the center position N_{centr} is

$$N_{centr} = \sum_{i=-200}^{200} N_i A_i / \sum_{i=-200}^{200} A_i, \quad (3)$$

N_i is the channel number, A_i is the amplitude of the channel N_i. At low polarizations the sign of the signal asymmetry is reversed and positions of $\delta 1$ and $\delta 2$ became unclear. Accessible data are fitted by the linear equations

$$\delta 1 \ [kHz] = 15.2 \cdot P_p, \ \delta 2 \ [kHz] = 29.4 \cdot P_p. \quad (4)$$

where polarization is given in relative units. On the other hand, the substitution of h=6.626·10^{-27} erg·s, γ_p=4257.7 Hz/G, N_p=9.09·10^{22} spin/cm^3 for ammonia density of 0.853 g/cm^3 at 77 K [7] and I_p=1/2 in Eq. 1 gives calculated displacement

$$\delta_{calc} \ [kHz] = \gamma_p \cdot H_{loc} = 34.3 \cdot P_p, \quad (5)$$

where we neglected a displacement owing to a small contribution from electron spins, seen in Fig. 2(b). Estimation by Eq. 5 gives a good agreement with $\delta 2$- displacement of signal maximum in Eqs. 4 but a disagreement with $\delta 1$-position of signal center. This disagreement was one of the reasons to re-investigate the same material [7] after ten years of storage at liquid nitrogen temperatures which decreased its electron concentration to about 10^{19} spin/cm^3. At lowered concentrations, the proton spectra can be subdivided into symmetrical fraction and a "residual" part, both seen in Fig. 3(a). Symmetrical fraction is induced by spins situated far-away from

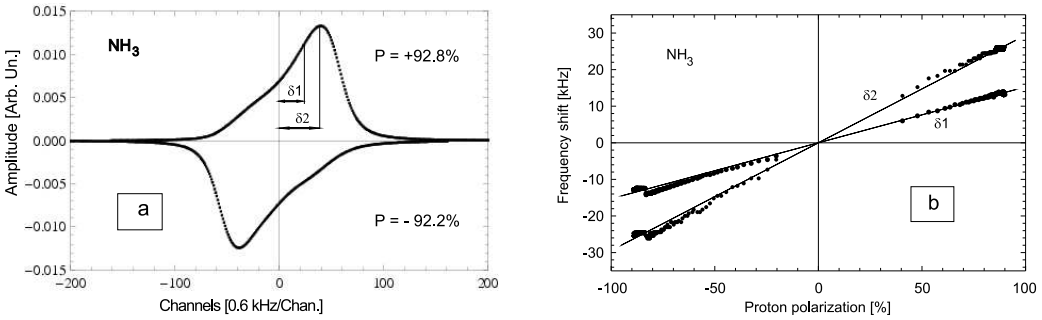

Fig. 2. a). Proton spectra of about ±90% polarizations. b). $\delta 1$ and $\delta 2$ are the data for center and maximum displacements and their fitting curves (see Eqs. 4) as a function of polarization; steps on the curve edges show a small contribution from electron spins seen after switching the MW power off.

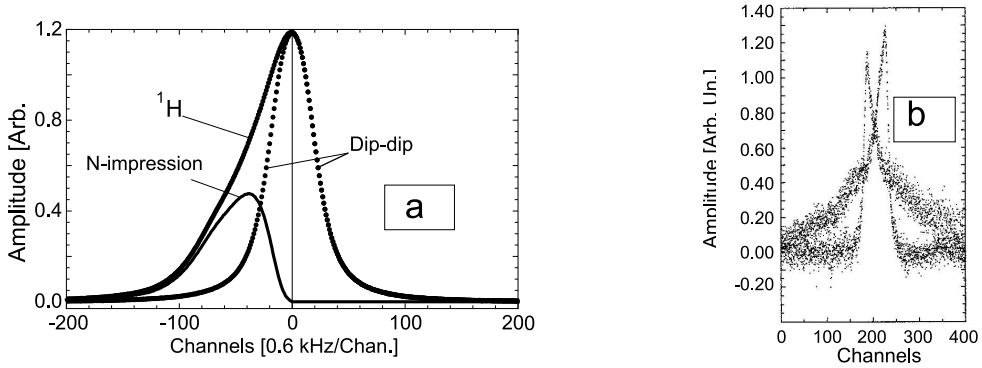

Fig. 3. a). Proton line in NH_3 ($P_p \approx$+92%) can be subdivided in a symmetrical part with dipolar interspin interactions and an "residual" part including also an indirect coupling between nitrogen and proton spins. b). The two measured parts of extremely broadened NMR nitrogen spectrum at +10% polarization, corresponding about the same spin temperature as for proton spectrum in Fig. 3(a). Unpolarized ^{14}N has an amplitude $1.3{\cdot}10^4$ worse compared with the proton [14].

paramagnetic centers, where the main interaction is owing to dipole-dipole interactions. Due to conservation of the dipolar energy at permutations of equivalent proton spins in ammonia molecules, spins of this fraction have to induce a symmetrical line-shape [8]. Their local field obeys to a linear dependence over the polarization [9], by the same way as $\delta 2$.

In contrast to the dipolar interaction, decreasing as r^{-3} with interspin distance r, the spins of the "residual" part undergo an additional shorter-acting indirect coupling through electron wave function. At weak coupling, their energy sublevels are [4,11]

$$E_{np} = -h\gamma_p(H_0 + H_{loc})m_p + hJ \cdot m_n m_p, \tag{6}$$

where J is a constant independent on the magnetic field as well as on an aggregate state of material [4], m_n=$< I_{zn} >$ and m_p=$< I_{zp} >$ are z-components of corresponding spins, proportional to their nuclear polarizations. J-term in Eq. 6 increases or decreases the spectral shift, depending on sign of the local field. At parallel spin orientation (m_p=1/2, m_n=1 or m_p=-1/2, m_n=-1), the proton energy will be increased by amount $hJ_{nm}/2$; for antiparallel (m_p=-1/2, m_n=1 or m_p=1/2, m_n=-1) the energy will be lowered by the same amount. In such a case, magnetic transitions obey the selection rule $\Delta(m_p + m_n)$=±1. Finally, at positive polarizations, this results to the two ν_{J-}, ν_{J+} unresolved transitions and ν_+ transition, in the order of increasing frequency (Fig. 1(b)) and the signal asymmetry is at lower frequency than the symmetrical part, see Fig. 3(a). For negative sign, we obtain ν_- and again ν_{J-} and ν_{J-} overlapping transitions in Fig. 1(b). In this case, J-term in Eq. 6 lead to an asymmetry at higher frequency than the symmetrical part, seen in the bottom curve in Fig. 2(a). Another

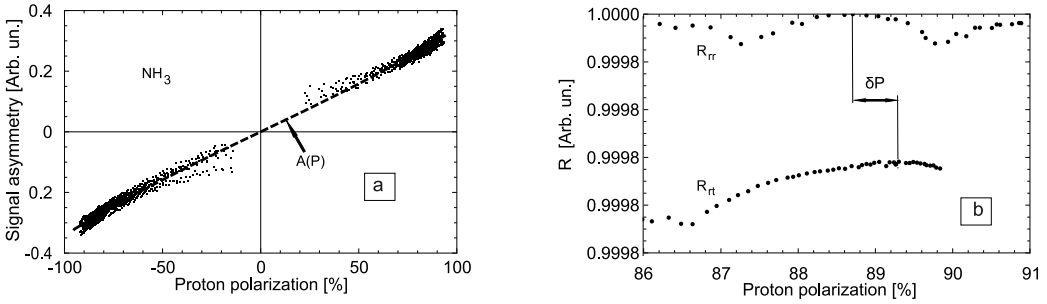

Fig. 4. (a). Amplitude of the asymmetrical part of spectra normalized to the unit area over polarization. (b). Correlation coefficients, see Eq. 8, over polarization; R_{rr}=1-the reference signal of 88.7% correlates with itself (top); R_{rt}-the same reference signal are compared with signals in different probe (bottom), δP shows the discrepancy of 0.7% between integral and asymmetry values obtained by cross-check.

allowed transition with m_n=0, in accordance with Eq. 6, contributes nothing to the signal asymmetry. Fig. 4(a) shows the approximate amplitudes of asymmetrical signals as a function of polarization for signal area normalized to one.

3.2 Comparison between NMR and impressed nitrogen spectra.

In an external magnetic field, the nitrogen spins ($I_n = 1$) have three magnetic sublevels $m_n = 0, \pm 1$, where m_n=$< I_{zn} >$, and the corresponding energies of these eigen-states are [12]

$$E_n = -h\nu_n m_n + h\nu_Q\{3\cos^2(\theta) - 1\}\{3(m_n)^2 - I(I+1)\} \approx -h\nu_n m_n \ , \qquad (7)$$

where the nitrogen Larmor frequency $\nu_n = \gamma_n H_0$ ≈7.7 MHz at 2.5 T field, $\nu_Q = (e^2qQ/h)/8$=-0.395 MHz for ammonia [13], eq is the nitrogen quadrupole moment and eQ is the value of the electrical field gradient along the principal axis of the field gradient tensor; θ is the angle between this axis and the direction of the magnetic field.

Detailed study of ^{14}N-spectra in the amorphous solid can be found in [7]. It was shown, that NMR line is extremely broadened by the random angle orientations and it can't be detected by Q-meter technique without displacement of the external field. Therefore, the left peak of ^{14}N NMR-spectrum, shown in Fig. 3(b) was measured at 2.45 T and the right peak was measured at 1.68 T both with 200 kHz sweep about the same central frequency of 6.47 MHz.

NMR-nitrogen spectra obey Δm_n=±1 selection rule but the proton asymmetry owing to J-term in Eq. 6 appears when $\Delta(m_p + m_n)$=±1 and $m_n \neq$0. The different selection rules explain the different signal-to-noise ratios between signals of about equal polarizations taken by the usual NMR (see Fig. 3(b)) and the nitrogen "impression" on the proton spectrum (see Fig. 3(a)). This difference comes by the fact that due to γ_p/γ_n ≈14≫1, the quadrupole term in Eq. 7 can be neglected. The quadrupole interactions have no actions on the proton asymmetry.

The "impression" strength is formed by the sum of ν_{J-} and ν_{J+} transitions (see Fig. 1(b)) whereas NMR intensities depend on difference between populations of the nearest Δm_n=±1 sublevels which are considerably less for rare and quadrupole nuclei with respect to the intensities of proton transitions. This explains the good advantage of the beam ionization for spectroscopy of the frozen dielectrics including biological substances. The first qualitative comparison between the indirect "impression" and routine NMR-nitrogen spectrum have been shown by their signal-to-noise ratios in Fig. 3(a, b).

4 Cross-checks of polarizations

As the first application, we have used the signal asymmetry for more accurate measurements of average polarizations in the three cell COMPASS target. On condition of an uniform material

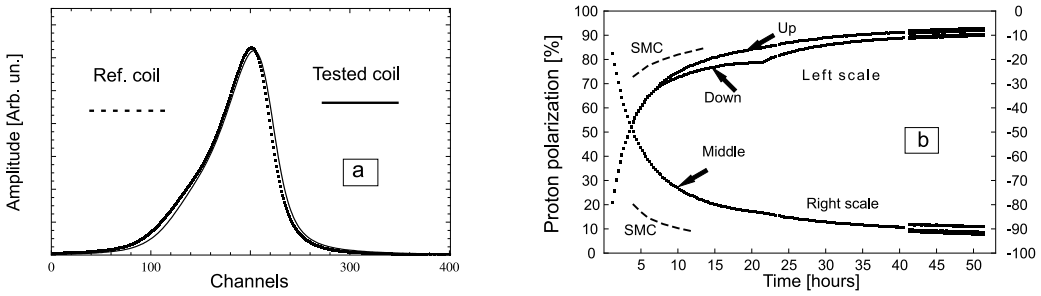

Fig. 5. a). Two spectra, slightly shifted for clarity sake, at maximum correlation. b). Build-up of the average polarizations in three-cell target which were measured with (3+4+3) probes. The end curves show all probe polarizations. Dashed SMC-curves demonstrate build-up for fresh material.

and external magnetic field, NMR spectra of equal proton polarizations must also have equal signal asymmetries. However in practice, the natural asymmetry are distorted by the nonuniformity of the target material and the external field and can also depend on the spectrometer resolution. For numeric comparison between line-shapes of A and B spectra, it is convenient to use the Pearson correlation coefficient

$$R = \frac{\sum_{i=1}^{N}(A_i - \overline{A})(B_i - \overline{B})}{\sqrt{\sum_{i=1}^{N}(A_i - \overline{A})^2 \sum_{i=1}^{N}(B_i - \overline{B})^2}}, \tag{8}$$

where A_i and B_i are amplitudes of i_th channel, $\overline{A}$ and $\overline{B}$ are the average amplitude of spectra; N is the maximum channel number.

The top curve in Fig. 4(b) demonstrates correlation coefficients between reference spectrum of 88.7% and the current spectrum of the same probe, taking during target polarization; R=1 is reached when the reference spectrum correlates with itself. The bottom curve shows correlation coefficients between the same reference spectrum of 88.7% and the current spectra but, this time, taking from the different testing probe. In the second case, the maximum of correlation coefficients should also mean of 88.7% polarization but its integral value in Fig. 4(b) separated by δP=0.7%. Fig. 5(a) shows these normalized spectra. Keeping in mind that a typical error for the thermal equilibrium (TE) calibration is about of $|\pm 1.5|\ \% > \delta$P=0.7%, one can slightly adjust the relative Q-meter calibrations staying whithin their absolute errors. Making the same comparison for all probes situated along the target length, it is possible to convert an additional information about asymmetry into more accurate relative polarizations in target cells. In particle experiments just these relative polarizations determine the particle asymmetries in scattering reactions. Fig. 5(b) demonstrates the build-up of the average polarizations in up-middle-down cells in the COMPASS target, detected by (3-4-3) probes, correspondingly. At the curve ends we plotted data from all ten probes after its mutual cross-checks. Data show a good spatial homogeneity of polarization as well as the high MW field uniformity in the three cell multimode cavity which provides of ±2% error bar in the COMPASS target.

5 Summary

Beam irradiation of crystalline ammonia originates the nuclear indirect spin-spin interactions acting over induced paramagnetic dopants. As a result, the original magnetic structure and the nuclear spectra of a material are transformed into the dipolar and the indirect parts. Owing to indirect coupling, the nitrogen spins create an “impression” on the proton spectra in the form of spectral asymmetry. This “impression” was found nearly independent on nitrogen quadrupole moment; it is mainly determined by energy sublevels having nonzero spin projection on the field direction. Experiment shows that the “impressions” have much better signal-to-noise resolution compared with that for nitrogen NMR-spectra. This property seems to be a very promising way

for the study of rare and quadrupole nuclei in dielectrics, including also biological structures. Further investigations need to be done for the better knowledge about its practical applications.

As for target technique, we have demonstrated the cross-checks between signal asymmetries and their integral proton polarizations using the Pearson correlation coefficient. The method allows to minimize the relative deviation of polarizations along the target for better accuracy in particle asymmetry measurement.

References

1. Editor G. R. Court, S. F. J. Cox, D. A. Cragg, T. O. Niinikoski, *Proc. of the 2_nd Workshop on Polarized Target Materials*. (Rutherford Appleton Lab., RL-80-080, October 1980) 1-146.
2. Editor W. Meyer, *Proc. of the 4_th Inter. Workshop on Polarized Target Materials and Techniques* (Universität Bonn, September 3-6, 1984) 13.
3. W. Meyer, Nucl. Instr.and Meth. in Phys. Res. **A 526**, (2004) 12-21.
4. H. S. Gutowsky, D. W. McCall and C. P. Slichter, J. Chem. Phys., **21**, (1953) 279.
5. W. Meyer at al., Nucl. Instr.and Meth., **A 215**, (1983) 65.
6. G. R. Court, at, al., Nucl. Instr.and Meth. **A 324**, (1993) 433.
7. B. Adeva et al., Nucl. Instr.and Meth., **A 419**, (1998) 60.
8. E. R. Andrew and R. Bersohn, J. Chem. Phys., **18**, (1950) 159.
9. A. Abragam and M. Goldman, Nuclear Magnetizm: Order and Disorder, (Clarendon Press, Oxford, 1982) **VII**.
10. Y. Kisselev et al., Nucl. Instr.and Meth., **A 526**, (2004) 105.
11. E. O. Stejskal and J.D. Memory, *High Resolution NMR in the Solid State* (Oxford University Press, 1994) 9.
12. W. de Boer,*Dynamic Orientation of Nuclei at Low Temperatures*, (Geneva, CERN, Yellow Report 74-11, Nuclear Physics Division, 13 May, 1974) 1-76.
13. S. S. Lehrer, C. T. O'Konski, J. Chem. Phys., **43**, (1965) 141.
14. G. R. Court et al., *Proc. of the 4_th Intern. Workshop on Polar. Target Materials and Techniques*, ed. W. Meyer, (Universität Bonn, September 3-6, 1984) 122.